

University of Groningen

## The role of small conductance calcium-activated potassium channels in mitochondrial dysfunction

Krabbendam, Inge

DOI:  
[10.33612/diss.144370526](https://doi.org/10.33612/diss.144370526)

**IMPORTANT NOTE: You are advised to consult the publisher's version (publisher's PDF) if you wish to cite from it. Please check the document version below.**

*Document Version*  
Publisher's PDF, also known as Version of record

*Publication date:*  
2020

[Link to publication in University of Groningen/UMCG research database](#)

*Citation for published version (APA):*  
Krabbendam, I. (2020). *The role of small conductance calcium-activated potassium channels in mitochondrial dysfunction: Targeting metabolic reprogramming and calcium homeostasis*. University of Groningen. <https://doi.org/10.33612/diss.144370526>

### Copyright

Other than for strictly personal use, it is not permitted to download or to forward/distribute the text or part of it without the consent of the author(s) and/or copyright holder(s), unless the work is under an open content license (like Creative Commons).

The publication may also be distributed here under the terms of Article 25fa of the Dutch Copyright Act, indicated by the "Taverne" license. More information can be found on the University of Groningen website: <https://www.rug.nl/library/open-access/self-archiving-pure/taverne-amendment>.

### Take-down policy

If you believe that this document breaches copyright please contact us providing details, and we will remove access to the work immediately and investigate your claim.

*Downloaded from the University of Groningen/UMCG research database (Pure): <http://www.rug.nl/research/portal>. For technical reasons the number of authors shown on this cover page is limited to 10 maximum.*

# Chapter 6

---

## Activation of SK channels regulates inflammatory processes in macrophages

*Manuscript in preparation*

Inge E. Krabbendam<sup>1</sup>, Rianne Kloosterman<sup>1</sup>,  
Christina H.T.J. van der Veen<sup>1</sup>, Martina Schmidt<sup>1</sup>, Amalia M. Dolga<sup>1</sup>

## Abstract

Activated macrophages undergo metabolic reprogramming, from oxidative phosphorylation towards glycolytic activities, which drives their pro-inflammatory phenotype. Increased mitochondrial oxidation of succinate and elevation of mitochondrial membrane potential drive mitochondrial reactive oxygen species (ROS) induced by reverse electron transport (RET), thereby potentiating the pro-inflammatory state. Recently, we have shown that potassium channels, in particularly small conductance calcium-activated potassium (SK) channels are able to mediate mitochondrial metabolic switches. Here, we aimed to study the role of SK channel activation on succinate-induced ROS-RET in inflammatory macrophages. Upon LPS-stimulated conditions, succinate increased cellular glycolytic capacity compared to LPS alone, while it did not further potentiate LPS-induced inflammation. In this study, we demonstrated that activation of SK channels reversed morphological changes upon macrophage activation. In addition, SK channel activation decreased LPS-induced *IL-1 $\beta$*  expression and cellular ROS production. Furthermore, SK channel activation reduced the LPS-mediated increase phagocytosis and glycolytic activity even in conditions potentiated by succinate.

## Introduction

Metabolic repurposing is crucial in regulating pro-inflammatory responses during macrophage activation. Upon activation, macrophage metabolism switches from oxidative phosphorylation (OXPHOS) to glycolysis, in order to maintain its mitochondrial membrane potential and prevent apoptotic cell death. This requires macrophages to initially adopt a pro-inflammatory phenotype and then later, when the immediate danger has passed, to acquire an anti-inflammatory phenotype to promote resolution and repair. A pro-inflammatory response can be initiated by lipopolysaccharides (LPS) binding and recognition, initiating NF- $\kappa$ B pathway activation (1). Activation of the NF- $\kappa$ B pathway leads to the formation of pro-inflammatory cytokines, such as interleukin-1 $\beta$  (IL-1 $\beta$ ) (2). Increased oxidation of succinate at complex II is a key regulator of the pro-inflammatory response to LPS, the stimulus that we use in our model, both through the generation of ROS following oxidation by the electron transport chain (ETC) and also via hypoxia-induced factor 1 $\alpha$  (HIF-1 $\alpha$ ) stabilization. Pro-inflammatory macrophages are more glycolytic, produce more ROS and accumulate succinate in larger amounts than resting macrophages (3). The increase in succinate concentrations can induce reverse electron transport (RET), when a part of the electrons flows through complex I in reverse direction. The production of O<sub>2</sub><sup>•</sup> at complex I by RET is evoked by a strongly reduced coenzyme Q (CoQ) pool and a high mitochondrial membrane potential, together providing the thermodynamic force to push electrons in reverse to the ROS-producing site within complex I, leading to a strong increase in O<sub>2</sub><sup>•</sup> production (4–6). These ROS produced via RET contribute to the expression of pro-inflammatory cytokines and increased HIF-1 $\alpha$  activity and expression (7,8). Hence, succinate oxidation by the ETC contributes to the pro-inflammatory response to LPS and links mitochondrial ROS to macrophage activation (7).

The shift in macrophages away from inflammatory gene expression towards anti-inflammatory gene expression is important, since an inflammatory environment (created in our experimental setting by LPS) dominates in inflammatory diseases. In addition, there are conditions in which IL-1 $\beta$  has been involved in the pathogenesis of auto-inflammatory diseases, that are characterized by local and systemic inflammation (9). Therefore, new strategies are necessary to prevent RET-induced increase in inflammation. Blocking ROS production with low concentrations of rotenone, specific complex I inhibitor,

inhibited this inflammatory phenotype, with RET at mitochondrial complex I as the origin of the pro-inflammatory ROS signal in LPS-activated macrophages (7). Mitochondrial complex I can generate ROS at two sites, i.e. the I<sub>Q</sub> and the I<sub>F</sub> site, during the forward transfer of electrons from NADH to CoQ (10). In normal situations, rotenone is a site I<sub>Q</sub> inhibitor that interrupts this electron transfer to CoQ and increases ROS production at site I<sub>F</sub> (11). However, when blocking the I<sub>Q</sub>-site of complex I with rotenone, the highly reduced CoQ pool that induces reverse electron transfer is blocked, thereby decreasing ROS production. The decrease in LPS-induced ROS with the complex I inhibitor rotenone is particularly interesting as rotenone lowers ROS by complex I if RET is occurring (12), and otherwise induces ROS production (11). Notably, other reports demonstrated that metformin, which inhibits complex I, decreased IL-1 $\beta$  in response to LPS (13), further emphasizing complex I dysfunction in inflammatory signalling. While additional work is required to assess the source of mitochondrial ROS during macrophage activation, ROS production at complex I via RET is an interesting candidate target.

Recently, we have shown that small conductance calcium-activated potassium (SK) channels play a role in mitochondrial ROS signalling and also in inflammation (14–16). SK channels belong to a large family of K<sup>+</sup> channels that are highly abundant in both the central nervous system and the peripheral nervous system (17–19). Calcium-activated potassium (K<sub>Ca</sub>) channels are expressed in a wide variety of tissues, including neuronal and cardiac cells, where they are involved in membrane potential regulation. K<sub>Ca</sub> channels are classified based on their Ca<sup>2+</sup> conductance, into large conductance (BK) and small conductance (SK) channels and intermediate conductance (IK) channels (20). Activation of any type of K<sub>Ca</sub> channels with pharmacological agents in pathological conditions is associated with protective effects, such as oxidative stress defense and DNA repair (21–23). Previous studies have shown that mitochondrial BK channel activation was able to reduce ROS-RET (24). In our lab, we have shown that pharmacological activation of mitochondrial SK channels with CyPPA was able to slightly decrease the activity of complex I in neuronal HT22 cells. In addition, CyPPA was able to significantly reduce LPS-stimulated inflammation in primary mouse microglia (14). During inflammation, macrophages in the periphery also play an important role. In this study, we wanted to investigate whether SK channel activation is able to reduce inflammation in macrophages, and whether it can inhibit ROS-RET at

mitochondrial complex I. We aimed to identify the role of SK channel activator CyPPA on succinate-induced ROS-RET in LPS-treated macrophages.

## Materials and Methods

### Cell culture and compounds

RAW 264.7 macrophages were cultured in Dulbecco's Modified Eagle Medium (DMEM) (Fisher Scientific; with 4.5 g/L glucose, GlutaMAX-I), 1 mM sodium pyruvate (Fisher Scientific), 2 mM L-Glutamin (Fisher Scientific), 10 µg/mL Gentamycin (Fisher Scientific), and 10% Fetal Bovine Serum (FBS; GE Healthcare Life Sciences) at 37 °C with 5% CO<sub>2</sub>. When indicated, cells were treated with diethylsuccinate, referred to as succinate (5-10 mM) (Sigma-Aldrich, Zwijndrecht, the Netherlands), rotenone (0.25 – 2 µM) (Sigma-Aldrich), CyPPA (5 – 50 µM) (provided by Prof. dr. F.J. Dekker, University of Groningen), and lipopolysaccharides (LPS) (5 ng/ml – 1 µg/ml) (Sigma-Aldrich).

### xCELLigence real-time impedance measurement

Macrophage activation was monitored in real-time with cell impedance measurements, using the xCELLigence system Real-Time Cell Analyzer RTCA-MP (Roche Diagnostics, Penzberg, Germany) as described previously (14). Cell index values were normalized to 1 at the time of the LPS application.

### Seahorse XF analysis

To analyze the shift in metabolism towards glycolysis in treated macrophages, a Seahorse extracellular flux assay was performed. On the day of the measurement, cells were pre-treated for 3 hours with succinate (5mM), CyPPA or the combination, followed by LPS treatment in the analyzer. The assay buffer contained base-medium (1x DMEM-powder (Sigma D5030), 143 mM NaCl, 3 mg/L Phenol red, pH 7.35), 1 mM sodium pyruvate, 2 mM L-Alanyl-L-Glutamine, and 0.4 mg/mL BSA, pH 7.35. After pre-treatment (3 h), the medium in the plate was replaced by assay buffer and cells were starved (without glucose) for 1 hour. The Seahorse XF Biosystem was used to assess the extracellular acidification rate (ECAR). Three baseline measurements (3x min mix, 0min delay, 3min measure = 3/0/3) were recorded followed by injection in port A with glucose (25 mM), with or without LPS (0.1 µg/ml), CyPPA (25 µM) or the combination. Measurements were recorded for 24 h (3/15/3). Immediately after analysis, protein content

was quantified using Pierce BCA Protein Assay Kit (Fisher Scientific). These data were then used to normalize the data obtained in the Seahorse analysis.

### **Quantitative real-time PCR**

RNA was isolated using TRIZOL reagent (TRI Reagent Solution, Applied Biosystems, the Netherlands) according to manufacturer's protocol. Total RNA yield was measured using the NanoDrop 1000Spectrometer (Thermo Fisher Scientific, Wilmington, DE, USA). Equal amounts of cDNA were synthesized using Reverse Transcription System (Promega, Madison, WI, USA), according to manufacturer's protocol. For qPCR, cDNA samples were mixed with SYBR green, forward primers, and reverse primers (see supplementary table 1). The qPCR was run on an Eco Real-Time PCR System (Illumina, CA, USA) and the protocol was as follows: 30 minutes polymerase activation at 95 °C. PCR cycling divided into 3 stages, denaturation for 30 minutes at 95 °C, annealing for 30 minutes at 54 °C and elongation for 30 minutes at 72 °C. The total cycle count was 45 cycles. Incubation lasted for 5 minutes at 72 °C. Finally, the melt curve was generated using the following protocol; 15 seconds at 95 °C, 15 seconds at 55 °C and a final 15 seconds at 95 °C. qPCR data were analyzed on LinRegPCR software.

### **Phagocytosis assay**

To determine the effect of the different compounds on the phagocytic activity of the cells, a phagocytosis assay was performed. Cytochalasin D (0.02 mM) (Sigma-Aldrich) was used as a positive control, and was added when the cells were seeded. RAW macrophages were pre-treated with or without rotenone or succinate (10 mM) in the presence or absence of CyPPA (25 µM), followed by LPS (0.1 µg/ml) (with or without CyPPA) treatment and pHrodo Red *S. aureus* BioParticles Conjugate (1 µg/0.1 ml) (Thermo Scientific, Massachusetts, USA, Cat no. A10010) and transfer of the plate into an IncuCyte S3 Live-Cell Analysis System (Essen BioScience, Michigan, USA) in a cell incubator (37°C, 5% CO<sub>2</sub>).. One image per well was taken every two hours for 72 hours using a 10x objective lens and then analyzed using the IncuCyte TM Basic Software. Red channel acquisition time was 800 ms. A mask was applied and the fluorescence signal was quantified from 4-6 technical replicates per condition. Data are shown until 48 hours and area under curve graph is calculated using GraphPad Prism software until 24 hours.



## Statistics

Data displayed are mean  $\pm$  SEM or mean  $\pm$  SD as indicated in the figure legends. Statistical analyses were carried out using Prism 5 (GraphPad Software, San Diego, USA) and statistical comparison was performed using one way ANOVA followed by Tukey's test for multiple comparisons. P values illustrating statistically significant differences between the mean values are defined as \* $p$ <0.05, \*\* $p$ <0.01, \*\*\* $p$ <0.001 compared to control, # $p$ <0.05, ## $p$ <0.01, ### $p$ <0.001 compared to LPS alone, \$ $p$ <0.05, \$\$ $p$ <0.01, \$\$\$ $p$ <0.001 compared to LPS + succinate.

**Table 1: Primer sequences**

Gene	Oligonucleotide Sequence (5' $\rightarrow$ 3')
<i>RPL13A</i>	F: AGAAGCAGATCTTGAGGTTACGG R: GTTCACACCAGGAGTCCGTT
<i>18S</i>	F: AAACGGCTACCACATCCAAG R: CCTCCAATGGATCCTCGTTA
<i>IL-1<math>\beta</math></i>	F: TGCCACCTTTTGACAGTGATG R: ATGTGCTGCTGCGAGATTTG
<i>SK2</i>	F: GAATGACCAAGCAAATACCCTAGT R: GTGACGATCCTTTTCTCAAAGTCT
<i>SK3</i>	F: GAAAAGAGAAAGCGACTGAGTGAC R: CATGGAATCCTTTGAGTACAAACC



## Results

### Activation of SK channels reverses morphological changes upon macrophage activation

We first established LPS-induced macrophage activation kinetics using real-time impedance measurements. These measurements provide information on morphological changes in real-time (25), which were continuously monitored for the whole period of LPS exposure. LPS is commonly used to induce activation of macrophages and in studies of bacterial infections (1). Impedance alterations were displayed as cell index. An increase in the cell index as assessed by xCELLigence indicates an increase of size of the macrophage cell (14). We have chosen 100 ng/ml for all further experiments since this concentration increased the cell index compared to lower concentrations and controls (Fig. 1A). All higher tested concentrations of LPS (100 ng/ml - 1 µg/ml) were able to strongly increase the cell index in similar levels to 100 ng/ml (Fig. S1B). Next, we assessed whether succinate pre-treatment can further increase the LPS-induced macrophage morphological alterations. Cells were pre-treated with succinate (5 mM, 3 hours), and the chosen concentration and time period were based on previous reports (7). The impedance measurements of the succinate pre-treatment followed by LPS challenge showed a comparable cell index compared to LPS alone. The cell index of succinate treatment alone was similar to that of the control. Next, we evaluated whether activation of SK channels with CyPPA in a pre- and co-treatment with succinate and LPS is able to either prevent or reduce the increase in the cell index that was mediated by succinate and LPS stimuli. LPS-challenged cells showed a lower cell index when treated in the presence of CyPPA (Fig. S1C). Notably, CyPPA reduced the increase in cell index even in the presence of succinate and LPS treatment in a dose-dependent manner (Fig. S1C). CyPPA 25µM was most similar to control (Fig. S1C), and strongly reduced the increase in cell index induced by succinate and LPS (Fig. 1B), thus this concentration was used in further experiments. A bar graph of the average cell index after 24 hours of cells treated with LPS in the presence or absence of succinate with or without CyPPA is shown in fig. S1E. CyPPA was shown to mediate its functions via SK2 and SK3 channels (26), therefore, we assessed and determined the gene expression of *KCNN2* (SK2) and *KCNN3* (SK3) in RAW macrophages (Fig. S1A).

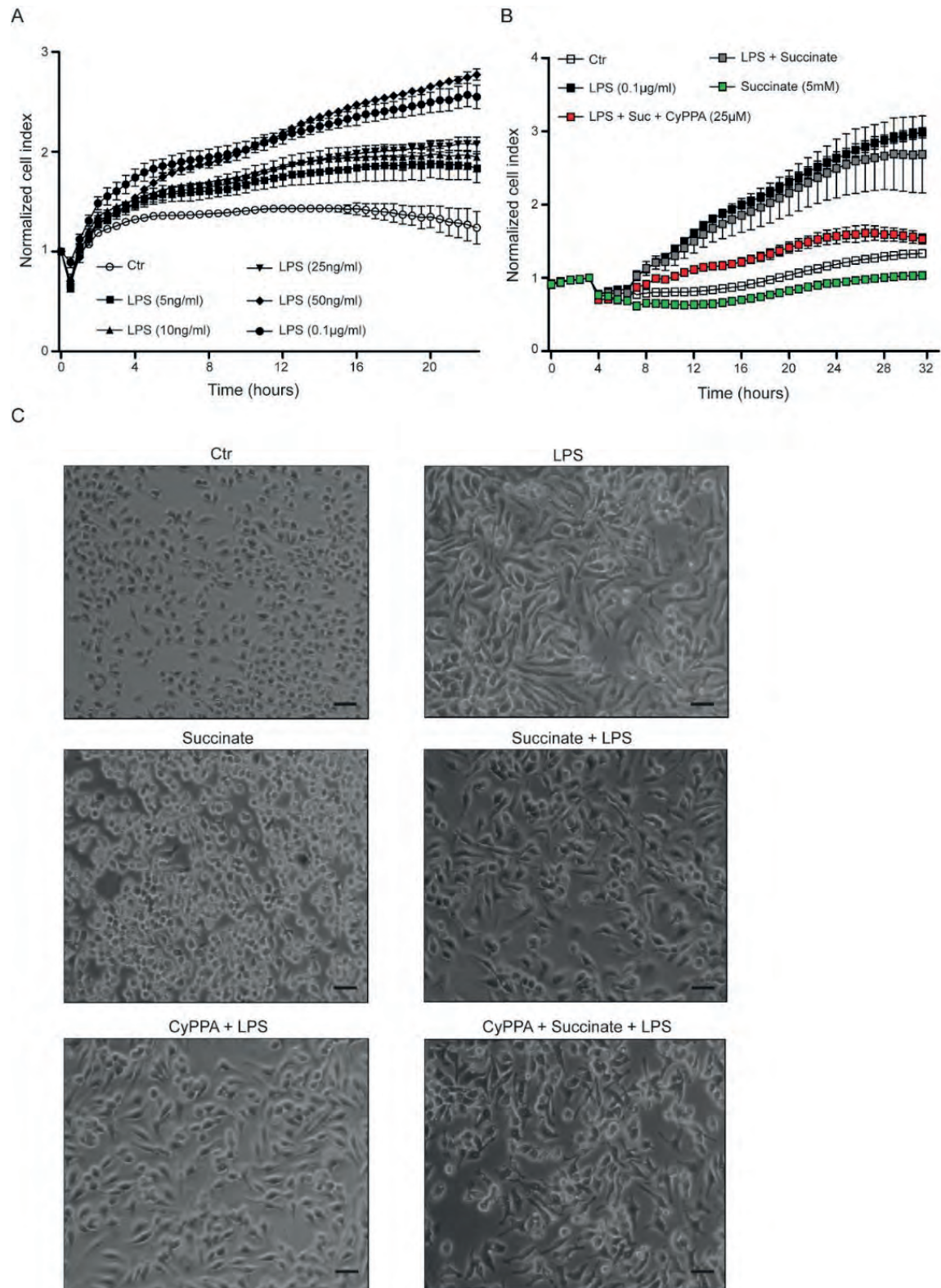


**Figure 1. Activation of SK channels reverses morphological changes upon macrophage activation.** (A, B) xCELLigence real-time impedance measurements of macrophages treated with different LPS concentrations (5 ng/ml - 0.1 µg/ml) (A) or treated with LPS (0.1 µg/ml) in the absence or presence of succinate (5 mM) with or without CyPPA (25 µM), or succinate alone (B). (C) microscopic images (10X magnification) of cells treated

for 24 h with LPS with or without CyPPA (25  $\mu$ M) co-treatment, preceded by 3 h succinate (5 mM) in the presence or absence of CyPPA (25  $\mu$ M). Scale bar is 100  $\mu$ M.

To further substantiate the real-time cell impedance measurements, we assessed morphometric alterations of macrophages under stimulated or physiological conditions also by microscopy (Fig. 1C). As shown in figure 1C, macrophages treated with succinate alone did not alter their morphology, while LPS challenge for 24 hours changed cell morphology. Pre-treatment of succinate following LPS stimulation altered the cells as well, but no obvious difference was observed compared to LPS alone. The combined treatment of CyPPA with succinate and LPS slightly altered the morphology and reduced the shape of the cells compared to LPS treated cells. These results showed that LPS is able to change and increase the shape of macrophages, while pre-treatment with succinate did not evidently change the morphological alterations mediated by LPS challenge.

Overall, these results suggest that succinate combined with LPS increase morphological shape of macrophages, and that CyPPA treatment reduced these structural modifications.

### **SK channel activation decreases LPS-induced IL-1 $\beta$ expression and ROS production**

LPS mediates macrophage activation and induces the expression of inflammatory markers, such as interleukin 1 beta (*IL1B*) genes responsible for IL-1 $\beta$  release. To further evaluate the contribution of SK channel activation on combined succinate and LPS-induced macrophage activation, we assessed changes in *IL1B* gene expression levels. Succinate is a well-established pro-inflammatory metabolite that is known to accumulate during macrophage activation, to levels that affect HIF-1 $\alpha$  activity, an important transcription factor in the expression of pro-inflammatory genes (27). Previously it was shown that succinate enhanced LPS-induced *IL1B* mRNA in bone marrow derived macrophages (BMDM) (7). In RAW macrophages, we observed that succinate (5 and 10 mM) did not further increase the LPS-induced *IL1B* mRNA expression. These mRNA expression levels were similar to the expression levels following LPS treatment (Fig. 2A and B). However, CyPPA co-treatment did reduce the *IL1B* mRNA expression induced by LPS and succinate pre-treatment. Next, we

assessed the effect of rotenone treatment. Rotenone alone, in low concentrations (0.25 – 1  $\mu$ M), had no toxic effects on the macrophages, both in the absence or presence of LPS, as measured by MTT assay (Fig. S1F). There was a trend towards a reduction in *IL1B* gene expression after rotenone pre-treatment before LPS stimulation.

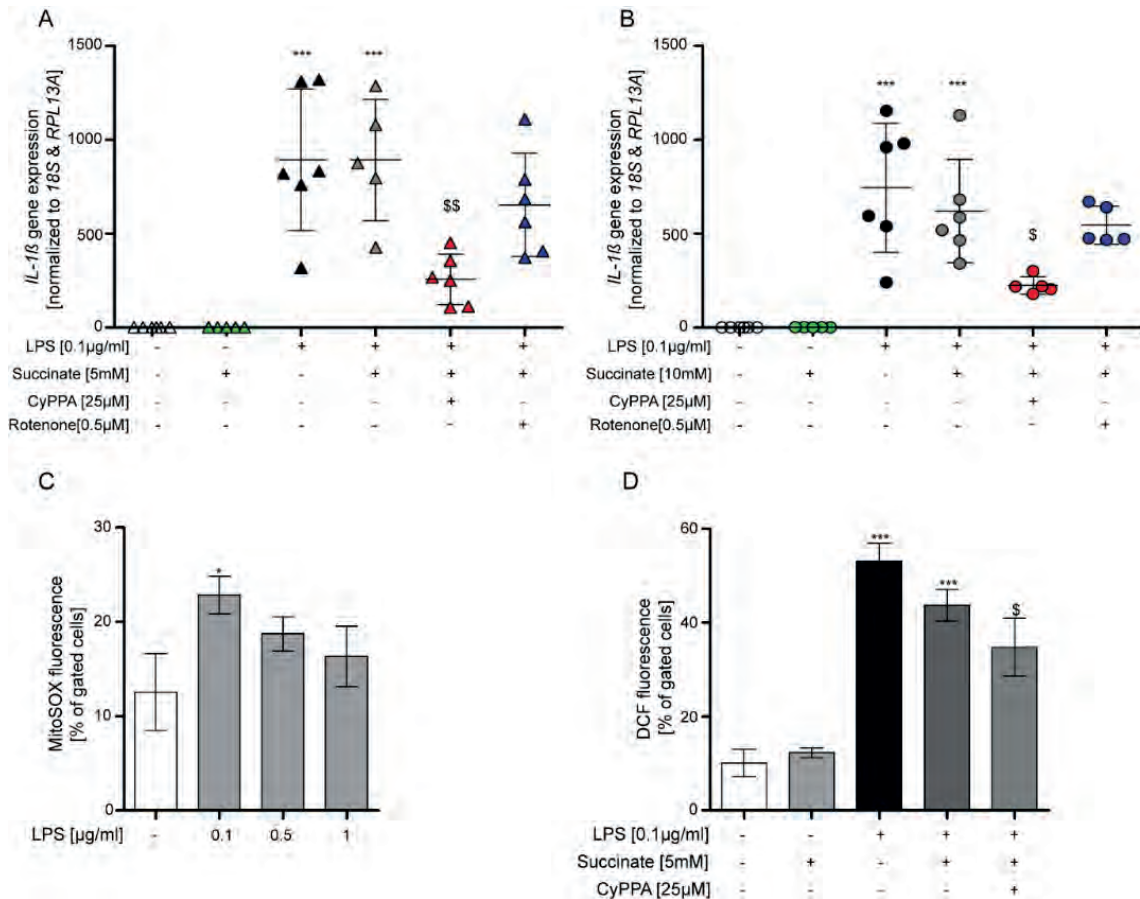


**Figure 2. SK channel activation decreases LPS-induced *IL-1 $\beta$*  expression and ROS production.** (A, B) *IL1B* gene expression, relative to 18S and RPL13A and normalized to control. Cells are treated with LPS (0.1  $\mu$ g/ml) alone (24 h), succinate alone (3 h) (5 mM (A) or 10 mM (B)), or LPS (24 h) pre-treated with succinate (3 h) with or without CyPPA pre- and co-treatment (25  $\mu$ M) or rotenone (0.5  $\mu$ M) pre-treatment, n=5-6 independent experiments. (C) MitoSOX fluorescence measuring mitochondrial superoxides, after treatment with different LPS concentrations (24 h) (0.1  $\mu$ g/ml – 1  $\mu$ g/ml). (D) cellular ROS ( $H_2$ DCFDA, depicted as DCF) measurements after treatment with LPS (0.1  $\mu$ g/ml) alone (24 h), succinate alone (3 h) (5 mM), or LPS (24 h) pre-treated with succinate (3 h), LPS pre-treated with succinate and pre- and co-treated with CyPPA (25  $\mu$ M). Data are presented as mean  $\pm$  SD; \* $p$ <0.05, \*\*\* $p$ <0.001, \$ $p$ <0.05, \$\$ $p$ <0.01, \*compared to control \$compared to LPS + succinate.



In contrast, *IL1B* gene expression was significantly reduced following CyPPA treatment (Fig. 2A and B). This may suggest that CyPPA, by inhibiting complex I, could inhibit succinate with LPS-induced increase in inflammatory processes, although other mechanisms might be involved as well.

Previous studies showed that blocking ROS production at complex I either pharmacologically or using genetic approaches, limited IL-1 $\beta$  levels and these approaches were protective against LPS, supporting a role for mitochondrial ROS production in inflammation (7). Therefore, we next studied ROS formation after LPS treatment. Addition of LPS led to an increase in ROS as measured by both mitoSOX and DCF (Fig. 2C and D). Mitochondrial ROS production as measured by mitoSOX was increased following LPS stimulation. We next studied cytosolic ROS levels. LPS significantly increased cellular ROS levels. Interestingly, succinate alone did not increase cytosolic ROS production (Fig. 2D). While pre-treatment of succinate before LPS had no additional effect on cytosolic ROS production, CyPPA co-treatment reduced cytosolic ROS levels induced by the succinate and LPS combined treatment.

In conclusion, these results indicate that CyPPA is potentially able to reduce the inflammation, possibly via its ability to attenuate ROS formation and subsequent IL-1 $\beta$  production.

### **LPS-induced increase in glycolysis potentiated by succinate can be reduced upon SK channel activation**

Upon activation, macrophages undergo a metabolic shift from oxidative phosphorylation to glycolysis (3). Here we studied whether this metabolic shift induced by LPS could be potentiated by succinate, and whether CyPPA was able to prevent this metabolic phenotype switch. The cells were pre-treated with succinate (5 mM) with or without CyPPA (25  $\mu$ M), followed by 24 h LPS (0.1  $\mu$ g/mL) treatment in the presence or absence of CyPPA. Glycolytic activity in macrophages was assessed by the Seahorse extracellular flux analyzer, that monitored extracellular acidification rate (ECAR) following the addition of various substances. These ECAR values indirectly correspond to the glycolytic activity and their analysis showed that LPS alone and CyPPA to a lesser extent increased the ECAR compared to control non-challenged macrophages (Fig. 3A). The results are also presented by area under curve measurements (Fig 3C and

D). The increase in ECAR may indirectly indicate increased glycolysis, as lactate is the primary source of free H<sup>+</sup> in the medium of cultured cells. In the same figure, it is shown that pre-treatment with succinate before LPS stimulation resulted in even higher ECAR values (Fig. 3A). When macrophages were treated with CyPPA in the presence of either LPS or LPS pre-treated with succinate, the ECAR is reduced to rates similar to the control (Fig. 3B).

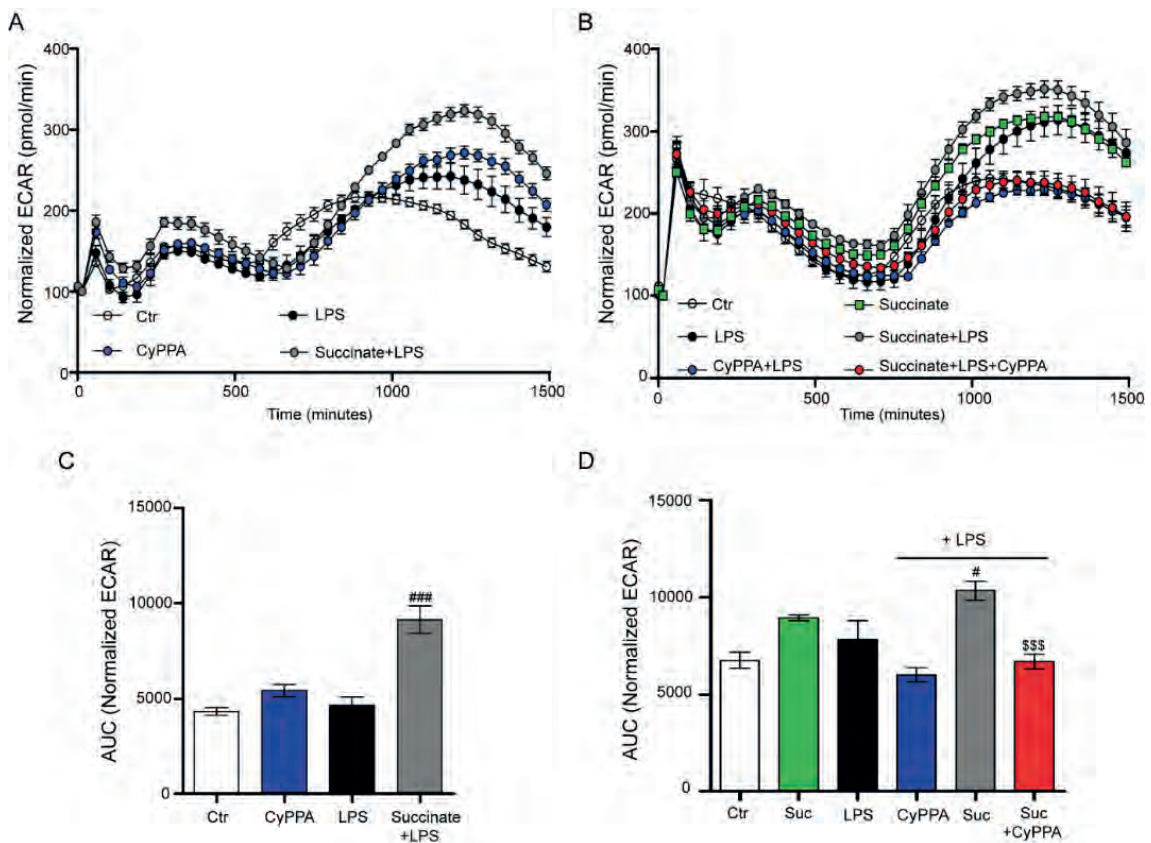


**Figure 3. SK channel activation reduces LPS-mediated increase in glycolysis potentiated by succinate.** (A-B) Representative experiment showing extracellular acidification rate (ECAR) in RAW macrophages pre-treated with succinate or normal medium following 3 baseline measurements, and injection in port A with LPS, CyPPA assay buffer with glucose alone (A) and the second graph pre-treatment with succinate, with or without LPS (24 h), with or without CyPPA pre- and co-treatment. In addition LPS alone and LPS + CyPPA pre- and co-treatment is shown (B). Data are presented as mean  $\pm$  SEM, data are normalized to protein content after experiment. (C-D) Area under curve (AUC) measurements of data corresponding with the graphs above. Data are presented as mean  $\pm$  SEM. #p<0.05, ###p<0.001, \$\$\$p<0.001, #compared to LPS alone, \$compared to LPS + succinate.

Cells that are switching away from OXPHOS to glycolytic metabolism are expected to have a higher mitochondrial membrane potential ( $\Psi_m$ ). This is because the  $\Psi_m$ , which is generated by proton pumping through the complexes of the mitochondrial inner membrane, is no longer being used by the ATP synthase to make ATP. We observed a reduction in the mitochondrial membrane potential as measured by TMRE fluorescence (Fig. S1G) in the presence of LPS and LPS pre-treated with succinate. CyPPA prevented against this reduction.

These results indicate that LPS increases glycolysis rates, whereas the presence of CyPPA was able to revert this effect. Moreover, treatment with succinate pushed the metabolism of the macrophages even further towards glycolysis in the presence of LPS, suggesting an effect of ROS-RET in the metabolic shift contributing to inflammatory conditions.

### **SK channel activation reduces phagocytosis**

Next, we aimed to study the effect of SK channel activation on LPS (+succinate)-induced inflammation on the functional level of phagocytosis. As shown in fig. 4, LPS-treated cells show slightly higher levels of phagocytosis compared to control non-stimulated macrophages. When macrophages were pre-treated with succinate followed by LPS challenge, the phagocytic activity was not significantly changed compared to LPS alone when measured at several time points (Fig. 4C). However, the overall phagocytic activity, as measured by area under curve for the first 24 hours, (Fig. 4B) was higher compared to control. In addition, co-treatment with CyPPA reduced the phagocytic activity. The representative images of the macrophages during the experiment at 0h and 24h are shown in fig. 4D. In summary, these results show that SK channel activation reduces phagocytosis in macrophages.



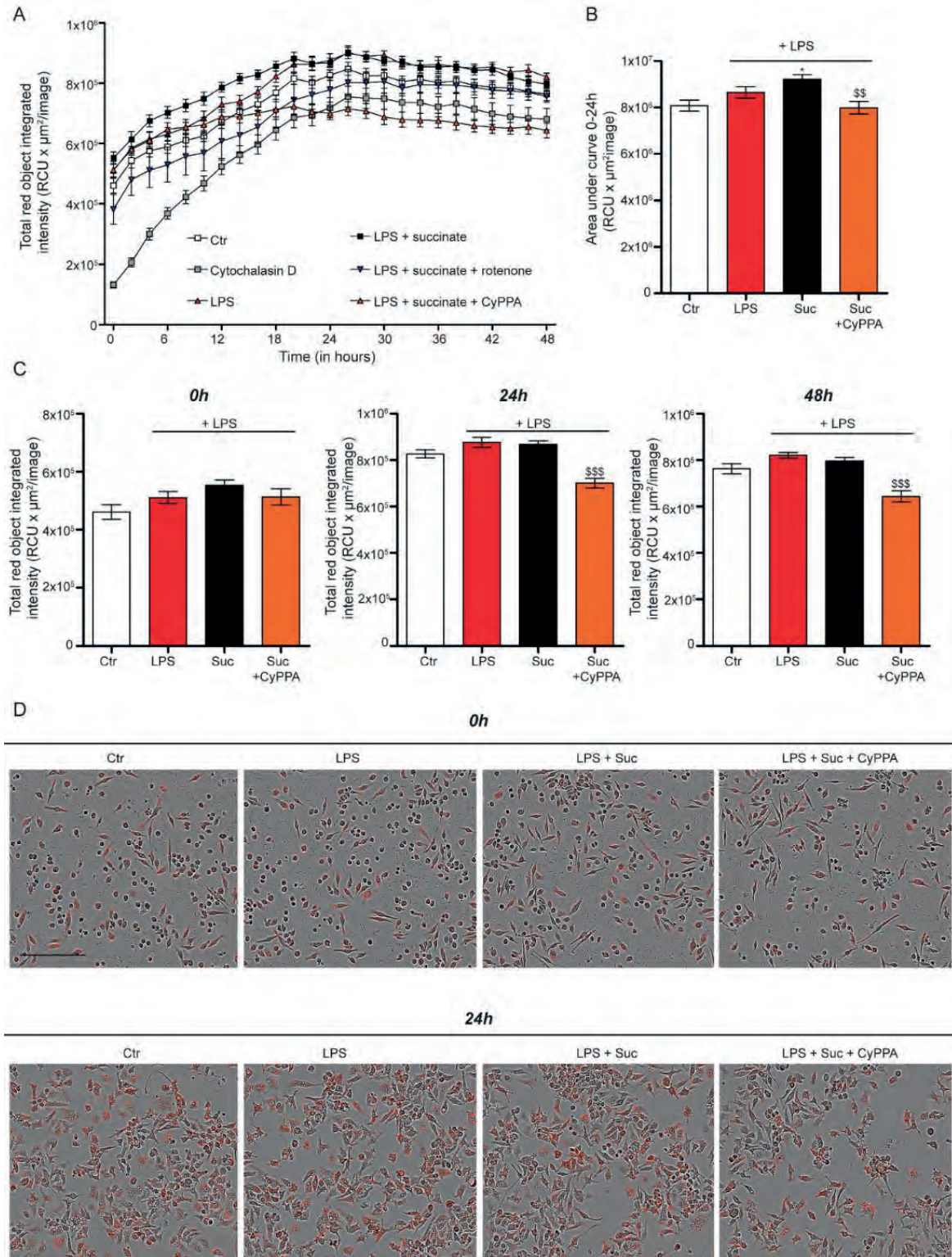


**Figure 4. Activation of SK channels attenuates phagocytosis.** (A) Phagocytosis assay using IncuCyte. The cells were pre-treated with succinate (5 mM) +/- CyPPA (25  $\mu\text{M}$ ) +/- Rotenone (0.5  $\mu\text{M}$ ), followed by 72 hour LPS treatment (0.1  $\mu\text{g}/\text{mL}$ ), (+/- CyPPA) in combination with 1  $\mu\text{g}/0.1$  ml pHrodo Red *S. aureus* BioParticles Conjugate. Images were taken every 2 hours, first image was 0-2 hours after the addition of the particles and

compounds. (B) corresponding area under the curve graph (0-24 hours). (C) data extracted at different time points (0 h, 24 h, 48 h). Data are presented as mean  $\pm$  SEM. \* $p < 0.05$ ,  $^{**}p < 0.01$ ,  $^{***}p < 0.001$ , \*compared to control,  $^{\$}$ compared to LPS + succinate. (D) Representative images of 0 h and 24 h following the start of the phagocytic assay. Scale bare represents 300  $\mu$ M.

## Discussion

The results of the present study demonstrate that in RAW macrophages, SK channel activation attenuates LPS-induced increases in morphological changes, cell proliferation, glycolytic activity, phagocytic activity and *IL1B* gene expression. Since previous studies showed that additional application of succinate could potentiate LPS activation via RET, we used this as a model to study CyPPA effects on this mechanism. Succinate is a well-established pro-inflammatory metabolite that is known to accumulate during macrophage activation, to levels that affect HIF-1 $\alpha$  activity, a key transcription factor in the expression of pro-inflammatory genes (27). Pre-treatment of LPS-activated BMDMs with succinate enhanced LPS-induced *IL1B* mRNA and pro-IL-1 $\beta$  protein with an accompanying boost in HIF-1 $\alpha$  protein levels (7,27). Succinate was also shown to boost LPS-induced glycolysis (7).

As shown by our bright-field microscopy and real-time impedance measurements, succinate did not enhance LPS-induced macrophage activation. Despite the obvious alteration in morphology following LPS treatment, it was difficult to detect small changes in morphology in the other treatment conditions. Morphology was also assessed by xCELLigence real-time impedance measurements. Similar to previous studies (14), LPS-induced macrophage impedance kinetic demonstrated LPS-altered macrophage morphological shape immediately following its application. In contrast to microscopic images, SK channel activation seemed able to reduce LPS (+succinate) - induced macrophage morphology alteration, findings that are in line with previous results showing that SK3 channel activation reduces LPS-dependent microglial activation (14). However, based on these results, succinate did not boost LPS induced morphological changes.

In previous studies succinate potentiated ROS production, which was shown to be critical for the consequent increase in IL-1 $\beta$  levels following LPS stimulation

(7). In the present study, we observed an increase in ROS generation as shown by mitochondrial and cytosolic ROS measurements in LPS-treated cells. In contrast to what has been shown previously (7), succinate did not potentiate LPS-induced mitochondrial ROS production (data not shown). High LPS concentrations may lead to an increased superoxide generation, but free superoxide radicals are rapidly converted to  $H_2O_2$  and  $O_2$ . This may explain why increased LPS concentrations and LPS combined with succinate did not lead to an increase in mitoSOX fluorescence, since the dye is selective for superoxides (28,29). The DCF staining results showed that combination treatment of succinate and LPS with CyPPA lead to reduced cellular ROS levels. Similarly, Mills and colleagues showed a decrease in LPS-induced ROS with the complex I inhibitor rotenone (7), suggesting that CyPPA might act via a similar mechanism. However, we did not observe the same boost in cellular ROS levels upon succinate with LPS stimulation as shown previously (7). One of the limitations of the DCF dye is that it does not directly react with  $H_2O_2$  (30). The probe preferred by most researchers when investigating ROS-RET generation at complex I is Amplex (Ultra)Red using isolated mitochondria. The dye reacts with horseradish peroxidase (HRP) -  $H_2O_2$  at a 1:1 ratio to form the fluorescent product resorufin (31). Superoxide ( $O_2^{\bullet}$ ) is the most upstream source of ROS formed within mitochondria, with most  $O_2^{\bullet}$  being rapidly converted to  $H_2O_2$  by manganese superoxide dismutase (MnSOD) within the matrix (32,33). Amplex (Ultra)Red is thus more specific in measuring ROS-RET formation at complex I, since  $H_2O_2$  formation reflects the reduction state of the CoQ pool, assuming that all  $O_2^{\bullet}$  are converted to  $H_2O_2$  by matrix MnSOD. Notably, ROS-RET production has also been shown to be attenuated by activation of large-conductance calcium-activated potassium (BK) channels in isolated guinea pig heart mitochondria (24). In addition, in our lab we previously have shown the inhibitory effect of CyPPA on mitochondrial complexes (unpublished data). Thus, the CyPPA effect on complex I - generated  $H_2O_2$  should be studied further using this method.

Since mitochondrial ROS, possibly produced by RET, drive expression of the cytokine  $IL-1\beta$  (7) we further investigated its gene expression under conditions of LPS (and succinate) in combination with CyPPA and rotenone. In general, LPS increased the gene expression, indicating that the macrophages were activated. However, succinate pretreatment before LPS did not further increase the expression of *IL1B*, contrary to the expectations. Interestingly, co-treatment with CyPPA decreased the gene expression. Rotenone pre-treatment also

decreased the gene expression, but not this was not significant. Possibly, this is due to the fact that we also co-treated the cells with CyPPA during LPS, and rotenone was only present during the succinate pre-treatment period. Investigation of protein levels and cytokine levels would provide more information.

We showed that CyPPA decreases LPS-induced IL-1 $\beta$ , possibly via inhibiting complex I. We next assessed the effects on metabolic shift, since it is an important mechanism during macrophage activation, and it has been shown that by blocking glycolytic activity, the IL-1 $\beta$  levels were also reduced (34). The same study revealed by metabolic screen and flux analyses that while there was an overall decrease in TCA cycle activity and mitochondrial respiration during LPS treatment, there was an accumulation of the TCA cycle intermediate succinate. In addition, succinate was able to enhance LPS-induced glycolysis (7) via stabilization of HIF-1 $\alpha$ , an important regulator of glycolytic metabolism. Indeed, we showed that LPS potentiated higher glycolytic activity. In line with previous studies, succinate further boosted the glycolytic activity in combination with LPS. Furthermore, SK channel activation reduced ECAR to levels similar to the control.

To assess macrophage function at a more functional level we also studied phagocytic activity. LPS-treated cells only showed a trend towards higher phagocytic activity compared to control.. Interestingly, previous reports have suggested LPS treatment as a possible explanation for decreased phagocytic capacity due to tolerance, observed in BMDMs, measured with the same assay as in our study (35). Succinate slightly potentiated the phagocytic activity upon pre-treatment before LPS stimulation. Treatment with CyPPA was able to reduce the phagocytic activity of the cells initiated by LPS with succinate. In addition, it has been shown that store-operated Ca<sup>2+</sup> channel inhibition diminished phagocytosis of *S. aureus* bacteria in control and LPS-treated cells (36).

It has been shown that SK channel activation reduces LPS-induced inflammation in microglia via attenuating intracellular calcium levels and nitric oxide release (14). Thus, the link between the ability of SK channel activation to reduce calcium, but also attenuate ROS production should be considered for future investigation. In addition, more information on the effects on mitochondrial membrane potential would be of interest in this topic, since it plays a role in ROS-RET and also in LPS-induced inflammation. Mild membrane depolarization



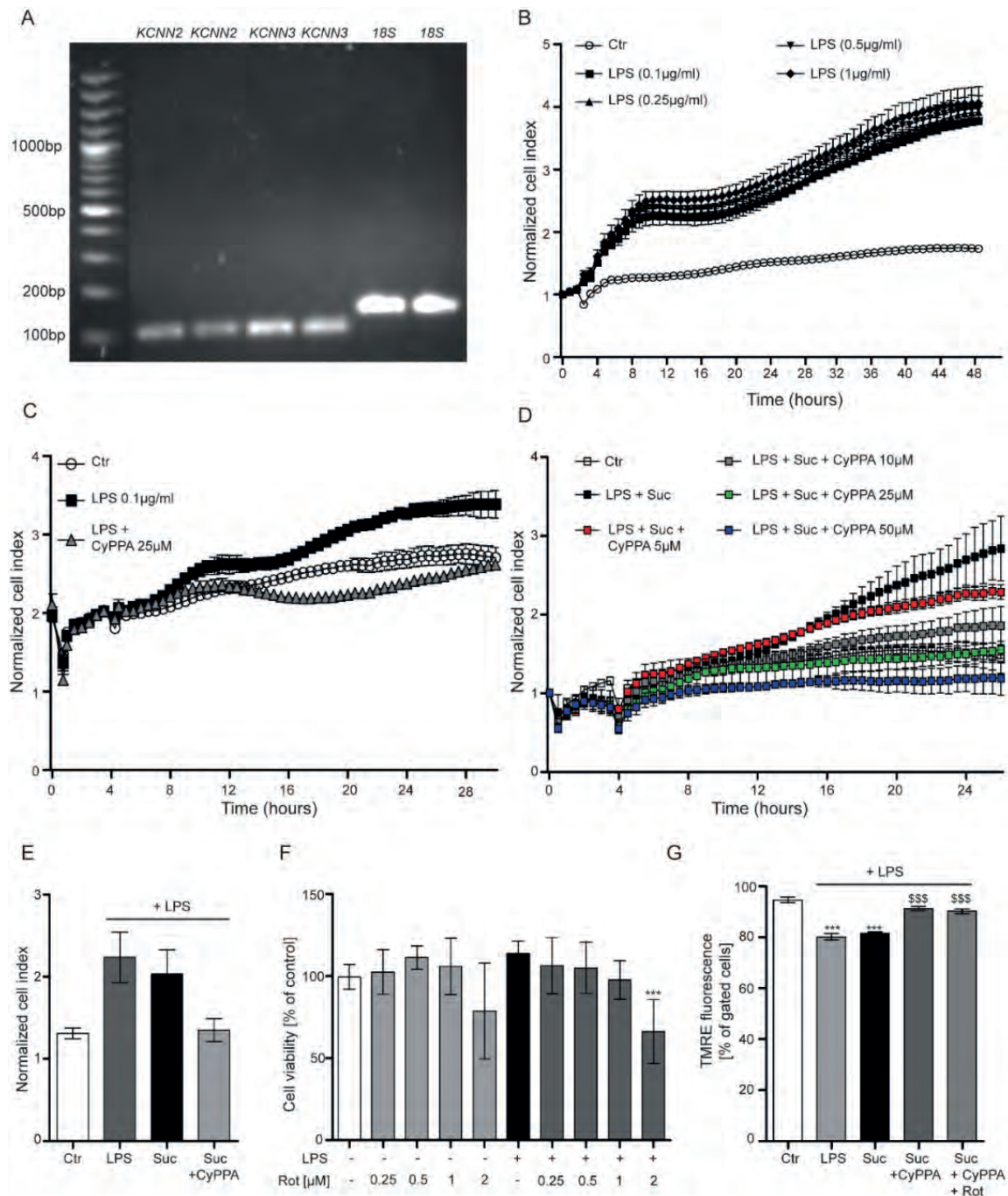
upon SK channel opening is something that has been observed before in other cell types (15). In rabbits, NS309, a pharmacological activator for SK channels attenuated spinal cord ischemia-reperfusion injury via decreasing oxidative stress and pro-inflammatory cytokines and preserving mitochondrial complex activities (16).

Importantly, the results of our study indicate that SK channel activation is able to reduce macrophage activity, thereby possibly reducing pro-inflammatory responses. Mechanisms involve reduced IL-1 $\beta$  production, attenuated glycolytic activity, and possibly via inhibition of complex I - produced ROS induced by RET. Therefore, targeting SK channels could be considered as a potential target for inflammatory diseases.

### **Acknowledgements**

The authors thank the Molecular Pharmacology group of University of Groningen for providing scientific and technical support during the experiments. A.M.D. is the recipient of a Rosalind Franklin Fellowship co-funded by the European Union and the University of Groningen.

## Supplementary figure



**Supplementary figure 1.** (A) Gene expression of KCNN2 and KCNN3 in RAW 264.7 macrophages. This figure shows the PCR product of KCNN2 (111bp), KCNN3 (111bp), and 18S (218bp). The primers were tested on untreated cells. (B) xCELLigence real-time impedance measurements of macrophages treated with different LPS concentrations (0.1 μg/ml – 1 μg/ml). (C) xCELLigence real-time impedance measurements of macrophages treated with LPS (0.1 μg/ml) or LPS + CyPPA (25 μM). (D) xCELLigence real-time impedance measurements of macrophages treated with succinate (10 mM) + LPS (0.1 μg/ml) and pre- and co-treated with different CyPPA concentrations (5 μM – 50 μM). (E) bar graph of the average cell index of the macrophage treatments with LPS

alone, LPS pre-treated with succinate, LPS pre-treated with succinate and pre- and co-treated with CyPPA from three independent xCELLigence experiments at time point 24 h (mean  $\pm$  SEM). (F) MTT assay of cells 3 hours pre-treated with rotenone (0.25 – 2  $\mu$ M) following LPS (0.1 $\mu$ g/ml) stimulation for 24 hours. (G) Mitochondrial membrane potential measurements by TMRE fluorescence after treatment with LPS (0.1  $\mu$ g/ml) alone (24 h), succinate alone (3 h) (5 mM), or LPS (24 h) pre-treated with succinate, LPS pre-treated with succinate and pre- and co-treated with CyPPA (25  $\mu$ M). MTT and TMRE data are presented as mean  $\pm$  SD. \* $p$ <0.05, \*\* $p$ <0.001,  $^{\$}$  $p$ <0.05,  $^{\$\$}$  $p$ <0.01, \*compared to control,  $^{\$}$ compared to LPS + succinate.



## References

1. Lu YC, Yeh WC, Ohashi PS. LPS/TLR4 signal transduction pathway. *Cytokine*. 2008;42(2):145–51.
2. Lawrence T. The nuclear factor NF-kappaB pathway in inflammation. *Cold Spring Harb Perspect Biol*. 2009;1(6):1–10.
3. O’Neill LAJ, Pearce EJ. Immunometabolism governs dendritic cell and macrophage function. *J Exp Med*. 2016;213(1):15–23.
4. Chance B, Hollunger G. The interaction of energy and electron transfer reactions in. *J Biol Chem*. 1961;236(5):1562–8.
5. Bentinger M, Tekle M, Dallner G. Coenzyme Q - Biosynthesis and functions. *Biochem Biophys Res Commun*. 2010;396(1):74–9.
6. Pryde KR, Hirst J. Superoxide is produced by the reduced flavin in mitochondrial complex I: A single, unified mechanism that applies during both forward and reverse electron transfer. *J Biol Chem*. 2011;286(20):18056–65.
7. Mills EL, Kelly B, Logan A, Costa ASH, Varma M, Bryant CE, et al. Succinate Dehydrogenase Supports Metabolic Repurposing of Mitochondria to Drive Inflammatory Macrophages. *Cell*. 2016;167(2):457-470.e13.
8. Mittal M, Siddiqui MR, Tran K, Reddy SP, Malik AB. Reactive oxygen species in inflammation and tissue injury. *Antioxidants Redox Signal*. 2014;20(7):1126–67.
9. CA D. Interleukin-1 in the pathogenesis and treatment of inflammatory diseases. *Blood*. 2011;117(14):3720–33.
10. Zhao RZ, Jiang S, Zhang L, Yu Z Bin. Mitochondrial electron transport chain, ROS generation and uncoupling (Review). *Int J Mol Med*. 2019;44(1):3–15.
11. Barrientos A, Moraes CT. Titrating the effects of mitochondrial complex I impairment in the cell physiology. *J Biol Chem*. 1999;274(23):16188–97.
12. Votyakova T V., Reynolds IJ.  $\Delta\psi_m$ -Dependent and -Independent Production of Reactive Oxygen Species By Rat Brain Mitochondria. *J Neurochem*. 2001;79(2):266–77.
13. Kelly B, Tannahill GM, Murphy MP, O’Neill LAJ. Metformin inhibits the production of reactive oxygen species from NADH: Ubiquinone oxidoreductase to limit induction of interleukin-1 $\beta$  (IL-1 $\beta$ ) and boosts interleukin-10 (IL-10) in lipopolysaccharide (LPS)-activated macrophages. *J Biol Chem*. 2015;290(33):20348–59.
14. Dolga AM, Letsche T, Gold M, Doti N, Bacher M, Chiamvimonvat N, et al. Activation of KCNN3/SK3/KCa2.3 channels attenuates enhanced calcium influx and inflammatory cytokine production in activated microglia. *Glia*. 2012;60(12):2050–64.
15. Richter M, Nickel C, Apel L, Kaas A, Dodel R, Culmsee C, et al. SK channel activation modulates mitochondrial respiration and attenuates neuronal HT-22 cell damage induced by H<sub>2</sub>O<sub>2</sub>. *Neurochem Int*. 2015;81:63–75.
16. Zhu J, Yang L-K, Chen W-L, Lin W, Wang Y-H, Chen T. Activation of SK/KCa Channel Attenuates Spinal Cord Ischemia-Reperfusion Injury via Anti-oxidative Activity and Inhibition of Mitochondrial Dysfunction in Rabbits. *Front Pharmacol*. 2019;10(April):1–12.
17. Sailer CA, Kaufmann WA, Marksteiner J, Knaus HG. Comparative immunohistochemical distribution of three small-conductance Ca<sup>2+</sup>-activated potassium channel subunits, SK1, SK2, and SK3 in mouse brain. *Mol Cell Neurosci*. 2004;26(3):458–69.
18. Rimini R, Rimland JM, Terstappen GC. Quantitative expression analysis of the small conductance calcium-activated potassium channels, SK1, SK2 and SK3, in human brain. *Mol Brain Res*. 2000;85(1–2):218–20.
19. Köhler AM, Hirschberg B, Bond CT, Kinzie JM, Marrion N V, Maylie J, et al. Small-Conductance , Calcium-Activated Potassium Channels from Mammalian Brain Published

- by : American Association for the Advancement of Science 2020;273(5282):1709–14.
20. Kaczmarek LK, Aldrich RW, Chandy KG, Grissmer S, Wei AD, Wulff H. International Union of Basic and Clinical Pharmacology . C . Nomenclature and Properties of Calcium-Activated and Sodium-Activated Potassium Channels. 2017;(January 2017):1–11.
  21. Krabbendam IE, Honrath B, Culmsee C, Dolga AM. Mitochondrial Ca<sup>2+</sup> -activated K<sup>+</sup> channels and their role in cell life and death pathways. *Cell Calcium*. 2017;69:101–11.
  22. Stowe DF, Aldakkak M, Camara AKS, Riess ML, Heinen A, Varadarajan SG, et al. Cardiac mitochondrial preconditioning by Big Ca<sup>2+</sup>-sensitive K<sup>+</sup> channel opening requires superoxide radical generation. *Am J Physiol Hear Circ Physiol*. 2006;53226:434–40.
  23. Frassdorf, J, Huhn R, Niersmann C, Weber NC, Schlack W, Preckel, B et al. Morphine induces preconditioning via activation of mitochondrial K<sub>Ca</sub> channels. *Can J Anesth*. 2010;57:767–73.
  24. Heinen AA, Aldakkak M, Stowe DF, Rhodes SS, Riess ML, Varadarajan SG, et al. Reverse electron flow-induced ROS production is attenuated by activation of mitochondrial Ca<sup>2+</sup>-sensitive K<sup>+</sup> channels. *Am J Physiol Heart Circ Physiol*. 2007;293(3):H1400–7.
  25. Diemert S, Dolga AM, Tobaben S, Grohm J, Pfeifer S, Oexler E, et al. Impedance measurement for real time detection of neuronal cell death. *J Neurosci Methods* [Internet]. 2012;203(1):69–77.
  26. Hougaard C, Eriksen BL, Jørgensen S, Johansen TH, Dyhring T, Madsen LS, et al. Selective positive modulation of the SK3 and SK2 subtypes of small conductance Ca<sup>2+</sup>-activated K<sup>+</sup> channels. *Br J Pharmacol*. 2007;151(5):655–65.
  27. Tannahill GM, Curtis AM, Adamik J, Palsson-Mcdermott EM, McGettrick AF, Goel G, et al. Succinate is an inflammatory signal that induces IL-1 $\beta$  through HIF-1 $\alpha$ . *Nature*. 2013;496(7444):238–42.
  28. Kauffman M, Kauffman M, Traore K, Zhu H, Trush M, Jia Z, et al. MitoSOX-Based Flow Cytometry for Detecting Mitochondrial ROS. *React Oxyg Species*. 2016;2(5):361–70.
  29. Robinson KM, Janes MS, Pehar M, Monette JS, Ross MF, Hagen TM, et al. Selective fluorescent imaging of superoxide in vivo using ethidium-based probes. *Proc Natl Acad Sci U S A*. 2006;103(41):15038–43.
  30. Kalyanaraman B, Darley-Usmar V, Davies KJA, Dennery PA, Forman HJ, Grisham MB, Mann GE, Moore K, Roberts II LJ IH. Measuring reactive oxygen and nitrogen species with fluorescent probes: challenges and limitations. *Free Radic Biol Med*. 2012;52(1):1–6.
  31. Quinlan CL, Perevoschikova IV, Goncalves RLS, Hey-Mogensen M BM. The Determination and Analysis of Site-Specific Rates of Mitochondrial Reactive Oxygen Species Production. *Methods Enzym*. 2013;526:189–217.
  32. Murphy MP. How mitochondria produce reactive oxygen species. *Biochem J*. 2009;417(1):1–13.
  33. Wong HS, Dighe PA, Mezera V, Monternier PA, Brand MD. Production of superoxide and hydrogen peroxide from specific mitochondrial sites under different bioenergetic conditions. *J Biol Chem*. 2017;292(41):16804–9.
  34. Tannahill G, Curtis A, Adamik J, Palsson-McDermott E, McGettrick A, Goel G, et al. Succinate is a danger signal that induces IL-1 $\beta$  via HIF-1 $\alpha$  GM. *Nature*. 2014;496(7444):238–42.
  35. Kapellos TS, Taylor L, Lee H, Cowley SA, James WS, Iqbal AJ, et al. A novel real time imaging platform to quantify macrophage phagocytosis. *Biochem Pharmacol*. 2016;116:107–19.
  36. Ye Y, Huang X, Zhang Y, Lai X, Wu X, Zeng X, et al. Calcium influx blocked by SK&F 96365 modulates the LPS plus IFN- $\gamma$ -induced inflammatory response in murine peritoneal macrophages. *Int Immunopharmacol*. 2012;12(2):384–93.

